# Spin decomposition of the responses of $^{44}$Ca and $^{48}$Ca to 300 MeV protons

F. T. Baker,[1] L. Bimbot,[2] R. W. Fergerson,[3] C. Glashausser,[3] A. Green,[3] O. Häusser,[4] K. Hicks,[5] K. Jones,[6] C. A. Miller,[5] M. Vetterli,[4] R. Abegg,[5] D. Beatty,[3] B. Bonin,[7] B. Castel,[8] X. Y. Chen,[9] V. Cupps,[3] C. Djalali,[10] R. Henderson,[5] K. P. Jackson,[5] R. Jeppesen,[4] K. Nakayama,[1] S. K. Nanda,[11] R. Sawafta,[12] and S. Yen[5]

[1]*University of Georgia, Athens, Georgia 30602*

[2]*Institut de Physique Nucleaire, F-91406 Orsay, France*

[3]*Rutgers University, Piscataway, New Jersey 08854*

[4]*Simon Fraser University, Burnaby, Canada V5A 1S6*

[5]*TRIUMF, 4004 Westbrook Mall, Vancouver, Canada V6T 2A3*

[6]*Los Alamos National Laboratory, Los Alamos, New Mexico 87544*

[7]*Centre d'Etudes Nucléaires de Saclay, 91191 Gif sur Yvette, CEDEX, France*

[8]*Queen's University, Kingston, Canada K7L 3N6*

[9]*University of Colorado, Boulder, Colorado 80309*

[10]*University of South Carolina, Columbia, South Carolina 29208*

[11]*Continuous Electron Beam Accelerator Facility, 12000 Jefferson Ave., Newport News, Virginia 23606*

[12]*University of Alberta, Edmonton, Canada T6G 2J1*

(Received 11 March 1991)

Angular distributions of the double-differential cross section $d^2\sigma/d\Omega\, dE(\sigma)$ and the spin-flip probability $S_{nn}$ have been measured for inclusive proton inelastic scattering from $^{44}$Ca at 290 MeV and from $^{48}$Ca at 318 MeV. Excitation energies up to about 50 MeV for $^{44}$Ca and 40 MeV for $^{48}$Ca have been investigated over the laboratory angular ranges of 3° to 12° for $^{44}$Ca and 3° to 9° for $^{48}$Ca. Multipole decompositions of angular distributions of both the spin-flip cross section $\sigma S_{nn}$ and the estimated cross section for $\Delta S=0$ transitions have been performed. Distributions of strengths were deduced for $\Delta L=1$, $\Delta S=0$ (the giant dipole), $\Delta L=2$, $\Delta S=0$ (the giant quadrupole), $\Delta L=0$, $\Delta S=1$ (the magnetic dipole), $\Delta L=1$, $\Delta S=1$ (the spin dipole), and $\Delta L=2$, $\Delta S=1$ (the spin quadrupole). The $\Delta S=0$ summed strengths for $^{44}$Ca are lower than for $^{40}$Ca and $^{48}$Ca. The spin-dipole summed strengths are found to be approximately independent of $A$. For $^{48}$Ca, essentially all $M1$ strength observed was in the 10.23 MeV $1^+$ state; for $^{44}$Ca, $M1$ strength was observed to be fragmented over a range of 7 to 18 Mev.

## I. INTRODUCTION

Until recently, studies of the nuclear continuum and of giant resonances using proton inelastic scattering were hindered by difficulties in determining the spin-transfer ($\Delta S$) decomposition of the measured cross sections. For example, the giant dipole (GDR) and giant quadrupole (GQR) resonances generally appear above an apparently featureless continuum; this has been treated as a smooth "background" which is then subtracted to obtain the resonance strengths. Virtually nothing was known about $\Delta S=1$ resonances or about the relative $\Delta S=1/\Delta S=0$ response of the continuum as a function of excitation energy ($\omega$) and momentum transfer ($q$). The advent of focal-plane polarimeters, however, has changed this situation. Now the spin-flip probability $S_{nn}$ can be measured along with the cross section $d^2\sigma/d\Omega\, d\omega(\sigma)$, and the spin decomposition of the "background" can be estimated. Under the assumption that $S_{nn}$ is relatively insensitive to such things as distortions, Fermi motion, relativistic effects, etc., the fraction of the total nuclear response which is due to $\Delta S=1$ transitions, $R_s$, has been shown [1,2] to be approximately determined by $S_{nn}$. At momentum transfer near 0.5 fm$^{-1}$ and for high $\omega(\geq 30$ MeV), $R_s$ has been determined [1–3] to be very large, more than 80%, for a wide range of targets and projectile energies. In the giant resonance region, the "background" has been shown [4] to be mostly $\Delta S=1$ strength with considerable resonance structure.

The spin-flip cross section $\sigma_{\rm SF}(\equiv\sigma S_{nn})$ is, to an excellent approximation, due only to $\Delta S=1$ transitions because $S_{nn}\approx 0$ for $\Delta S=0$ transitions at intermediate energies. A recent paper [5] describes the analysis of $\sigma_{\rm SF}$ for a 319-MeV proton scattering from $^{40}$Ca. There, the first clear determination of the distribution of spin-dipole strength relative to sum-rule predictions was described and a spin-dipole resonance (SDR) approximately exhausting the sum rule was observed. Similar multipole decompositions for $^{54}$Fe have been performed [6] which deduce both SDR and $M1$ strength distributions. Here, similar analyses are presented for $^{44}$Ca and $^{48}$Ca; the summed SDR strength is found to be quite independent of $A$ for the calcium isotopes.

For $\Delta S=0$ transitions there is no simple cross section with contributions only from $\Delta S=0$ transitions analogous to $\sigma_{\rm SF}$ for the $\Delta S=1$ transitions. The cross section for $\Delta S=0$ transitions only may be written [4] as

$$\sigma_0=\sigma-(\sigma_{\rm SF}/\alpha)\ , \tag{1}$$

 

where $\alpha$ is the spin-flip probability for the $\Delta S=1$ transitions. Clearly, then, $\alpha$ is model dependent and depends on the nucleon-nucleon ($NN$) force, the nuclear structure, and the reaction mechanism. While considerable progress is being made [7] in random-phase-approximation/distorted-wave impulse-approximation (RPA/DWIA) calculations, sophisticated estimates of $\alpha$ are not presently available. Previous results for GDR and GQR strengths in $^{40}$Ca [5] and $^{54}$Fe [6] assumed that $\alpha$ may be determined approximately from the appropriately isospin-averaged free $NN$ force (determined from the Love-Franey $t$ matrix [8,9]). The analyses presented here for $^{44}$Ca and $^{48}$Ca are also based on this assumption. The $\Delta S=0$ summed strengths for $^{44}$Ca are found to be surprisingly smaller than for $^{40,48}$Ca.

## II. EXPERIMENTAL DETAILS

The $^{44}$Ca$(\vec{p},\vec{p}\,')$ experiment was performed at TRIUMF using the medium-resolution spectrometer (MRS) and an incident proton energy of 290 MeV. The $^{48}$Ca$(\vec{p},\vec{p}\,')$ experiment was performed at LAMPF using the high-resolution spectrometer (HRS) and an incident proton energy of 318 MeV. The details of the focal-plane polarimeters and of the experimental facilities have been previously described [10–12].

For $^{44}$Ca, the MRS focal-plane acceptance permitted acquisition of data for energy loss $\omega$ up to approximately 50 MeV with a single magnetic field setting at each scattering angle. The target, enriched to 98.78% of $^{44}$Ca, had a thickness of 53.5 mg/cm$^2$. Data were acquired for laboratory scattering angles 3°, 5°, 7°, 9°, and 12° ($q=0.26$, 0.38, 0.50, 0.64, and 0.84 fm$^{-1}$ at $\omega=20$ MeV). Absolute normalization of the $\sigma$ data was achieved from the knowledge of the target thickness and integrated beam current; the uncertainty is estimated at 10%. The cross-section data were taken at a later time than the spin-flip probability data which presented the following problem: a change in hardware made acquisition of $\sigma$ data at 3°, an angle where $S_{nn}$ had been measured, not possible. Absolute cross sections at 3° were therefore estimated by linearly extrapolating measured cross sections at 3.5° and 4.5°.

$S_{nn}$ data were also measured for $\omega$ up to about 80 MeV in $^{44}$Ca for $\theta=7°$ in order to verify that $R_s$ remains large with increasing $\omega$. These data have been published [2] and will not be discussed here.

For $^{48}$Ca, four magnetic-field settings per scattering angle were required to obtain data for the approximate energy loss range of 6 MeV $\leq\omega\leq$ 40 MeV. The target, enriched to 99%, was 150 mg/cm$^2$ thick. Data were obtained at laboratory scattering angles of 3°, 5°, 7°, and 9° ($q=0.26$, 0.39, 0.53, and 0.67 fm$^{-1}$ at $\omega=20$ MeV). The absolute normalization of the data was somewhat more problematical than for $^{44}$Ca because the size of the target was small enough that the entire beam did not strike it. However, careful comparison of yields for the four energy bites at each angle show that *relative* cross sections could be reliably measured. The elastic-scattering yields were therefore measured at small angles and absolute normalization was achieved by normalizing these to an optical model calculation at 318 meV for $^{48}$Ca using the experimentally determined [13] optical model parameters for 334-MeV proton scattering from $^{40}$Ca. This procedure yielded cross sections for the 10.23-MeV $1^+$ state which were in excellent agreement with previous measurements [14,15].

## III. SYSTEMATIC FEATURES OF DATA FOR Ca ISOTOPES

Shown by the dots (triangles) in Figs. 1–5 are the data for the cross section $\sigma$, the spin-flip probability $S_{nn}$, the spin-flip cross section $\sigma_{SF}$, the approximate cross section for $\Delta S=0$ transitions $\sigma_0$, and the analyzing power $A_y$, respectively, for $^{44}$Ca ($^{48}$Ca). The relative spin responses $R_s$, determined from the $S_{nn}$ data, are shown in Fig. 6. Examination of Figs. 1–6 reveals interesting comparisons between $^{44}$Ca and $^{48}$Ca. Figure 1 shows that $\sigma$ is, for the most part, larger for $^{48}$Ca than $^{44}$Ca in the giant resonance region around $\omega\sim20$ MeV; the $\sigma$ data [5] for $^{40}$Ca are quite similar to those of $^{48}$Ca. However, differences in $S_{nn}$ (Fig. 2) are such that $\sigma_{SF}$ (Fig. 3) is, except for low $\omega$ at 3°, virtually identical for both nuclei. As will be discussed in Sec. V B below, the reason for the difference in the low $\omega$ data at 3° is the different distribution of M1 strength in the two nuclei. Thus the differences in $\sigma$ are

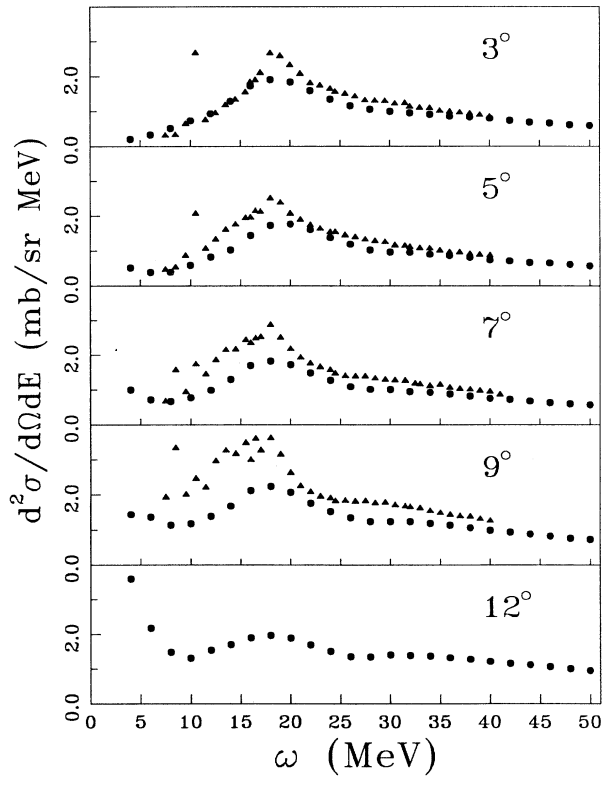


FIG. 1. Spectra of double-differential cross sections for the $^{44}$Ca$(\vec{p},\vec{p}')$ reaction at $E_p=290$ MeV (dots) and the $^{48}$Ca$(\vec{p},\vec{p}')$ reaction at 318 MeV (triangles). Spectra are labeled by laboratory scattering angles.

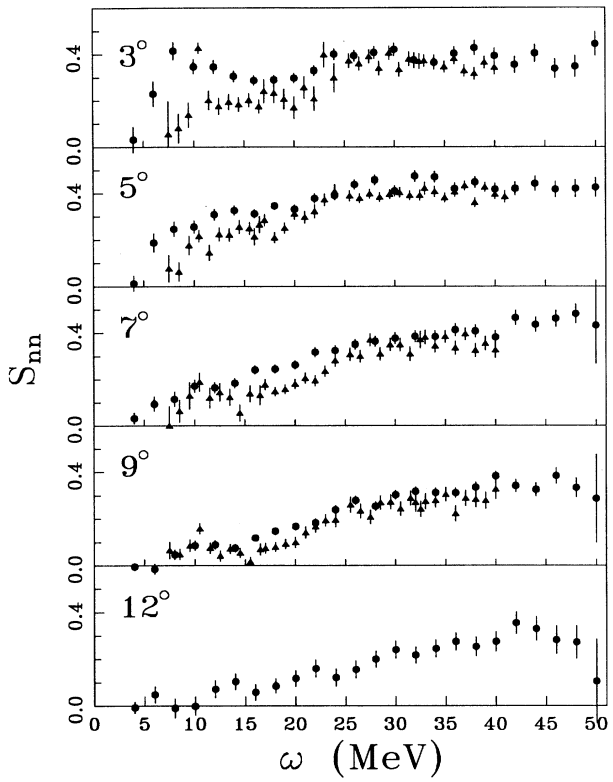


FIG. 2. Spectra of spin-flip probabilities presented as in Fig. 1.

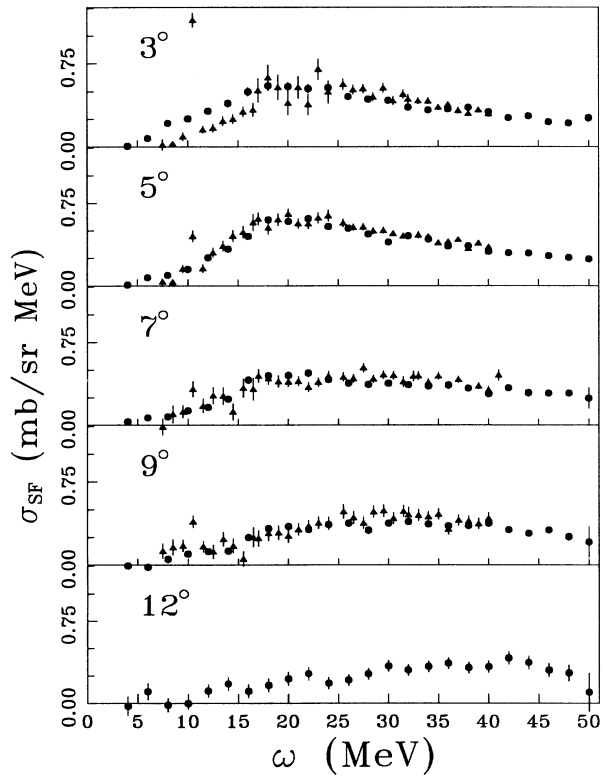


FIG. 3. Spectra of spin-flip cross sections presented as in Fig. 1.

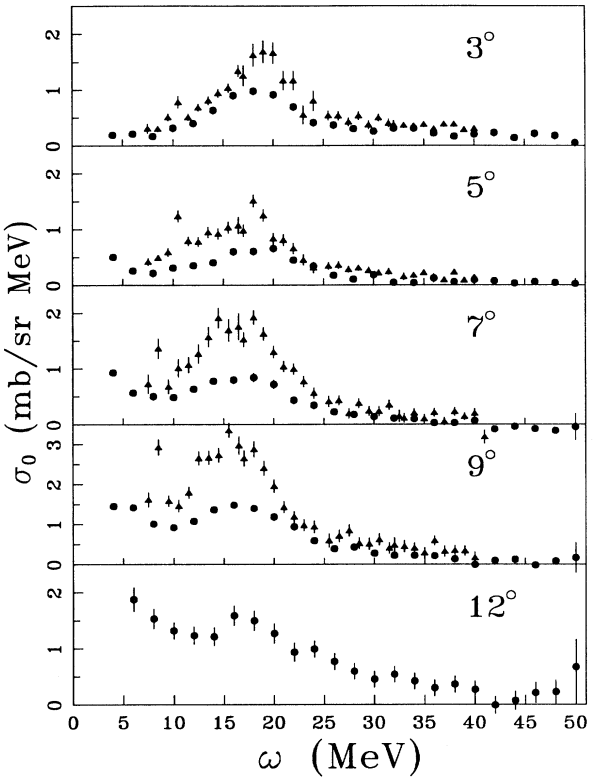


FIG. 4. Spectra of approximate $\Delta S=0$ cross sections presented as in Fig. 1.

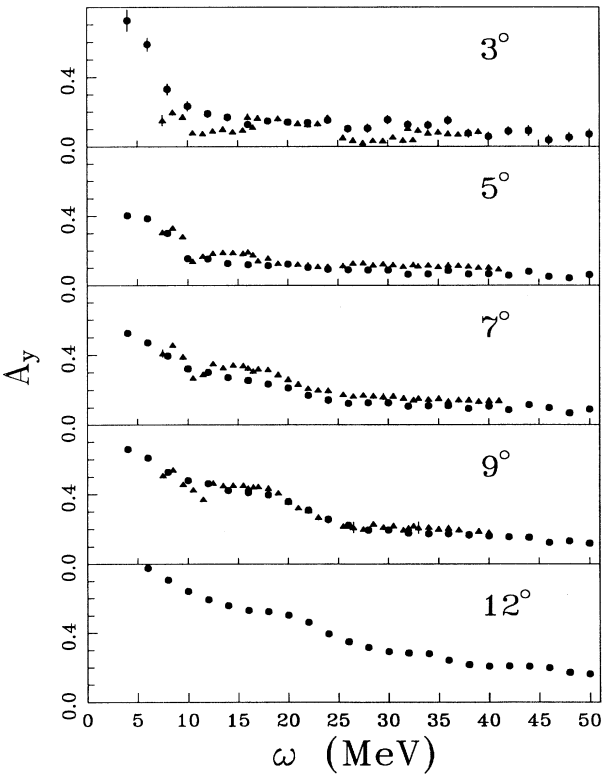


FIG. 5. Spectra of analyzing powers presented as in Fig. 1.

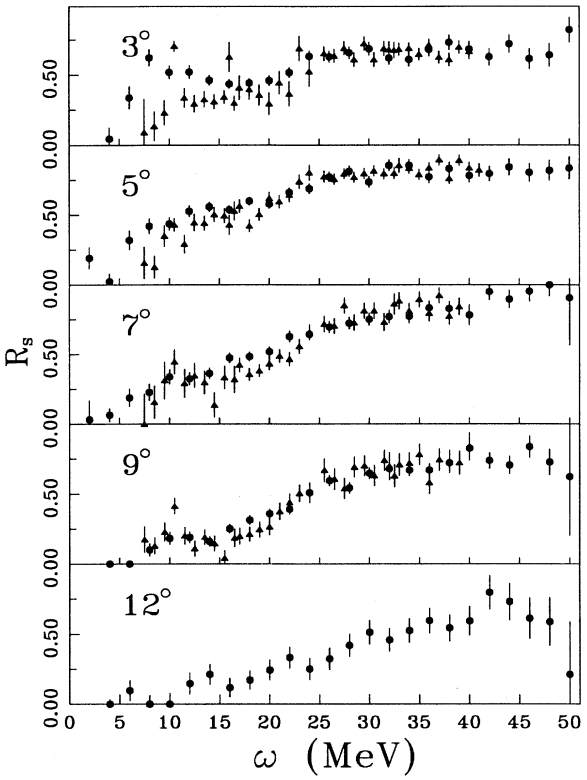


FIG. 6. Spectra of relative spin responses presented as in Fig. 1.

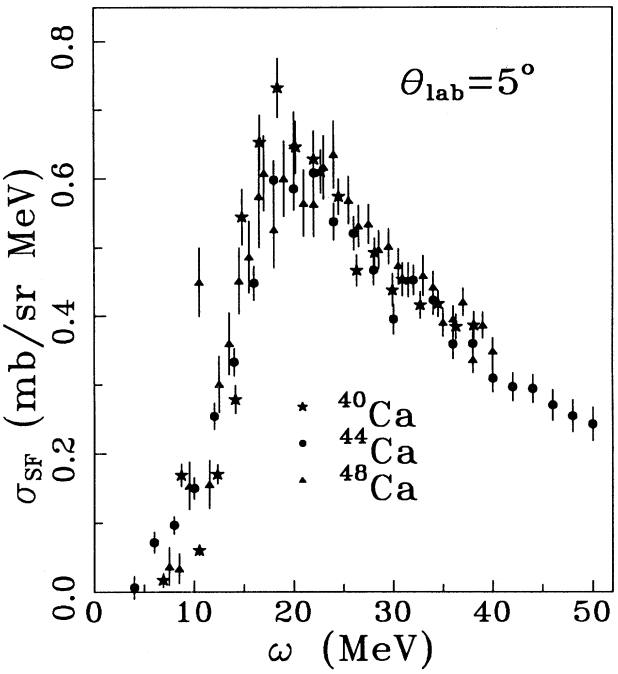


FIG. 7. The spin-flip cross section spectra for $^{40}$Ca, $^{44}$Ca, and $^{48}$Ca at a laboratory scattering angle of 5°.

apparently due mainly to differences on $\sigma_0$ (Fig. 4). These large differences will obviously have significant impact on the deduced strengths for the $\Delta S=0$ transitions as will be seen in Sec. V A below. It is difficult to understand this discontinuity in $\sigma_0$ between $^{44}$Ca and $^{48}$Ca.

Except at low $\omega$ at 3°, the values of $R_s$ determined from the $S_{nn}$ data for $^{44}$Ca and $^{48}$Ca are very similar to each other as illustrated in Fig. 6. In the giant resonance region, where $\Delta S=0$ correlations are expected to be dominant, $R_s$ is still only slightly less than 0.5 at most angles. At high excitation, $R_s$ rises to 0.80 and larger. These features have been seen in $^{40}$Ca and a number of other nuclei, as discussed recently in Ref. [2].

Shown in Fig. 7 are the spectra of $\sigma_{SF}$ for $^{40}$Ca, $^{44}$Ca, and $^{48}$Ca at a laboratory scattering angle of 5°; spectra at other angles are comparably similar. This constancy of $\sigma_{SF}$, is, at first, surprising, for two reasons. First, data for the $^{40}$Ca$(p,n)$ reaction [16] has continuum cross sections which are approximately half those for the $^{48}$Ca$(p,n)$ reaction. Second, one would expect the addition of eight $f_{7/2}$ neutrons to the $A=40$ core to have a significant impact on the inelastic scattering of protons. However, some reflection allows a qualitative understanding of the $(p,p')$ and $(p,n)$ data. No $(p,n)$ transitions possible from the $^{40}$Ca core will be blocked by adding neutrons but new transitions from the $\nu f_{7/2}$ orbital will become possible; therefore the cross section for $(p,n)$ should increase as neutrons are added. For $(p,p')$, however, adding $\nu f_{7/2}$ particles will block some transitions possible in $^{40}$Ca, thereby decreasing the cross section; an added cross section due to new transitions from the $\nu f_{7/2}$ orbital evidently balances this loss of cross section. It is interesting that the schematic model, described in Sec. IV B and in Ref. [5], predicts near constancy for the cross sections for all three Ca isotopes.

These qualitative arguments are further corroborated by our continuum RPA calculations for $^{40}$Ca and $^{48}$Ca. The technique that we have adopted is similar to the one described in detail by Bertsch and Tsai [17] which is based on a coordinate space representation of the Green functions. The method has been widely adopted since it is easily amenable to the use of the Skyrme interactions. Briefly, the first step is a calculation of the unperturbed Green function as a function of excitation energy, $\omega$, from the Hartree-Fock wave functions $\phi_h$. The results of this calculation are used to generate the RPA Green function. The transition density for giant excitations of spin character at a particular excitation energy is then determined from the imaginary part of the RPA Green function. The calculations predict a ratio of cross sections for $^{40}$Ca$(p,n)/^{48}$Ca$(p,n)$ of 0.56 in good agreement with experiment [16] an near equality for the $^{40}$Ca$(p,p')$ and $^{48}$Ca$(p,p')$ cross sections, quite consistent with our results and schematic-model calculations.

## IV. ANALYSIS

### A. Analysis of $\sigma_0$ data

The $\sigma_0$ data were analyzed in a manner similar to that described in Ref. [4]. Angular distributions for a given

angular momentum transfer $L$ were calculated using ECIS79 with the optical potential of Ref. [13] at an arbitrary $\omega_L$ for 100% exhaustion of the energy-weighted sum rule (EWSR) at $\omega_L$. These calculations used a macroscopic model for the excitation, including the full Thomas spin-orbit term, Coulomb excitation, equal deformations for all potentials, and relativistic kinematics. The GDR calculations were done as in Ref. [4]; the isovector potential was determined by scaling the optical potential using the volume integrals of the two-body interaction in the isovector and isoscalar channels as obtained using the Love-Franey $t$ matrix [8,9]. The strengths of the contributing multipoles were determined by fitting $\sigma_0(q)$ of each energy bin with a $\chi^2$ minimization routine. This routine calculates search errors which include the effects of correlations among the parameters; it is these errors which are shown in figures showing extracted strengths. As in Ref. [4], angular distributions for $\Delta L=1$, $\Delta L=2$, and $\Delta L=4$ were used, since our data do not have sufficient angular range to reliably separate $\Delta L=2$ and $\Delta L=3$; the angular distributions predicted for $^{48}$Ca for $\omega_L=20$ MeV and 100% exhaustion of the EWSR are shown in Fig. 8(a). No significance can be attributed to the extracted $\Delta L=4$ strength which is assumed to simulate contributions from all multipoles with $\Delta L\geq 3$. Monopole transitions were neglected since there is evidence [18,19] that they are weak in this region, and, in any case, they would be very difficult to distinguish from the GDR. If extraordinarily large GDR strengths are deduced, one possible explanation could be contributions from monopole strength. The calculated angular distributions (as functions of momentum transfer since $q$ depends on $\omega$ as well as $\theta$) were used but multiplied by $\omega_L/\omega$ so that the resulting summed strength represents the fraction of the EWSR exhausted.

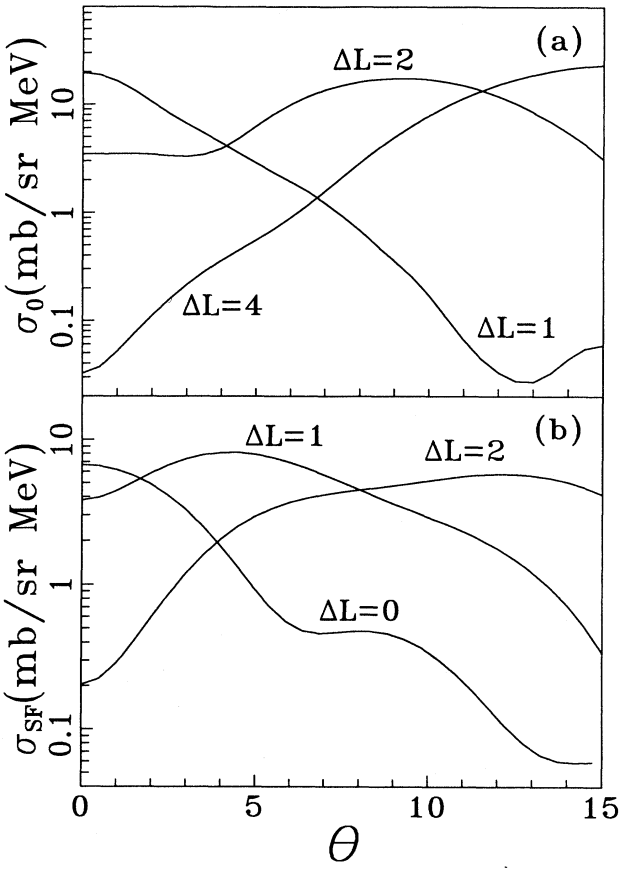


FIG. 8. Angular distributions used in the multipole decompositions of $^{48}$Ca. $\Delta S=0$ transitions are shown in (a), $\Delta S=1$ transitions are shown in (b).

### B. Analysis of $\sigma_{SF}$ data

Analysis of $\sigma_{SF}$ data here is very similar to the analysis of $^{40}$Ca data previously described [5]. There an extended version of the schematic model of Boucher *et al.* [20] was used. For a $\Delta S=1$ transition with $\Delta L=L$, $\Delta J=J$, and $\Delta T=T$, $\sigma_{SF}$ can be written in terms of the nucleon-nucleon $t$ matrix:

$$[\sigma_{SF}(q)]_{L,J,T}=N\left\{D_T^t|F_T(q)|^2\left|\left\langle J\left|\sum_i \boldsymbol{\sigma}_i\cdot\hat{\mathbf{Q}}(\delta_{T0}+T\tau_{iz})e^{i\mathbf{q}\cdot\mathbf{r}_i}\right|0\right\rangle\right|^2\right.$$
$$\left.+D_T^l|E_t(q)|^2\left|\left\langle J\left|\sum_i \boldsymbol{\sigma}_i\cdot\hat{\mathbf{q}}(\delta_{T0}+T\tau_{iz})e^{i\mathbf{q}\cdot\mathbf{r}_i}\right|0\right\rangle\right|^2\right\}. \quad (2)$$

where

$$\hat{\mathbf{q}}=(\mathbf{k}-\mathbf{k}')/|\mathbf{k}-\mathbf{k}'|\ , \quad (3)$$

$$\hat{\mathbf{Q}}=(\mathbf{k}+\mathbf{k}')/|\mathbf{k}+\mathbf{k}'|\ , \quad (4)$$

$E_T$ and $F_T$ are the longitudinal and transverse coefficients of the Love-Franey $t$-matrix [8,9] and $D_T^{t,l}$ are approximate corrections for distortion effects. The normalization factor, $N$, was calculated relativistically as in Ref. [5].

The matrix elements in Eq. (2), which are $L$ and $J$ dependent, were calculated as in Ref. [20]:

$$\left|\left\langle J\left|\sum_i \sigma_i\cdot\hat{\mathbf{Q}}e^{i\mathbf{q}\cdot\mathbf{r}_i}\right|0\right\rangle\right|^2 = A_L b_J\left[\int r^{L+1}j_L(qr)\frac{d\rho}{dr}dr\right]^2, \tag{5}$$

$$\left|\left\langle J\left|\sum_i \sigma_i\cdot\hat{\mathbf{q}}e^{i\mathbf{q}\cdot\mathbf{r}_i}\right|0\right\rangle\right|^2 = A_L C_j\left[\int r^{L+1}j_L(qr)\frac{d\rho}{dr}dr\right]^2. \tag{6}$$

Here, $\rho$ is the nucleon density and taken to be a three-parameter Fermi distribution,

$$\rho(r)=\rho_0(1+wr^2/c^2)/\{1+\exp[(r-c)/a]\}\ , \tag{7}$$

where $\rho_0$ is chosen such that

$$4\pi\int\rho r^2dr = A\ . \tag{8}$$

For $^{48}$Ca the results [21] from electron scattering were used, $w=-0.3$ fm, $c=3.7369$ fm, and $a=0.5245$ fm. For $^{44}$Ca we used $w=-0.0569$ fm, $c=3.7027$ fm, and $a=0.5524$ fm determined by interpolating between $^{40}$Ca and $^{48}$Ca electron-scattering results [21].

The factors $D_T^{l,t}$ of Eq. (2) used to approximate the effects of distortion were assumed to be the same as those determined [5] for $^{40}$Ca, 0.735, 0.200, 0.171, and 0.227 for $D_1^l$, $D_1^t$, $D_0^l$, and $D_0^t$, respectively.

As in Ref. [5], only spin-dipole ($L=1$, $J^\pi=0^-,1^-,2^-$) and spin-quadrupole ($L=2$, $J^\pi=1^+,2^+,3^+$) states have been included in the calculations. The constants $A_L$ are, for 100% exhaustion of the EWSR, given by

$$A_L=\frac{(4\pi)^2}{\omega_L m A}\times\begin{cases}\frac{1}{2}, & L=1\\ 1/\langle r^2\rangle, & L=2\end{cases} \tag{9}$$

where $\omega_L$ is the energy of the resonance and

$$\langle r^2\rangle = 4\pi\int\rho r^4dr\ . \tag{10}$$

The constants $B_J(C_J)$ are $0,\frac{1}{2},\frac{1}{2},\frac{1}{10},\frac{1}{2}$, and $\frac{2}{5}$, ($\frac{1}{3}$, 0, $\frac{2}{3}$, $\frac{2}{5}$, 0, and $\frac{3}{5}$) for $J^\pi$ of $0^-$, $1^-$, $2^-$, $1^+$, $2^+$, and $3^+$, respectively.

There are three revisions which must be implemented for $^{44}$Ca and $^{48}$Ca. The first of these revisions is required because the Suzuki [22] sum rules are valid only for spin-saturated nuclei. Suzuki [23] has given expressions for corrections for the sum rules for the case of spin-dipole transitions: the sum-rule sums should be multiplied by $1+\delta(J^\pi)$ where

$$\delta(0^-)=2\delta(1^-)=-2\delta(2^-) = \frac{2}{3A}\sum\langle 0|\boldsymbol{l}\cdot\mathbf{s}|0\rangle\ . \tag{11}$$

Assuming $L$-$S$ coupling, $\delta(0^-)$ is 0.182 for $^{44}$Ca and 0.333 for $^{48}$Ca. We then multiplied the calculations by the appropriate factors $1+\delta(J^\pi)$. This correction leaves the sum $\sigma(0^-)+\sigma(1^-)+\sigma(2^-)$, which is used in the fitting of our data, almost unchanged. No corrections of this type were made for the spin-quadrupole calculations.

The second required revision relates to the relative contributions of isoscalar and isovector transitions to the total cross sections. In Ref. [5], $\Delta T=0$ and $\Delta T=1$ cross sections were simply added; this is appropriate for a $T=0$ nucleus like $^{40}$Ca. However, for $^{44}$Ca and $^{48}$Ca, the appropriate isospin average must be performed:

$$[\sigma_{\rm SF}(q)]_{L,J}=N\left\{|F(q)|^2\left|\left\langle J\left|\sum_i\sigma_i\cdot\hat{\mathbf{Q}}e^{i\mathbf{q}\cdot\mathbf{r}_i}\right|0\right\rangle\right|^2+|E(q)|^2\left|\left\langle J\left|\sum_i\sigma_i\cdot\hat{\mathbf{q}}e^{i\mathbf{q}\cdot\mathbf{r}_i}\right|0\right\rangle\right|^2\right\}. \tag{12}$$

The isospin-averaged $t$ matrix coefficients in Eq. (12) are given by

$$|E(q)|^2=D_1^l|E_1(q)|^2+D_0^l|E_0(q)|^2 -2(N-Z)\sqrt{D_1^lD_0^l}\ \mathrm{Re}[E_0(q)E_1^*(q)]/A \tag{13}$$

and

$$|F(q)|^2=D_1^t|F_1(q)|^2+D_0^t|F_0(q)|^2 -2(N-Z)\sqrt{D_1^tD_0^t}\ \mathrm{Re}[F_0(q)F_1^*(q)]/A\ . \tag{14}$$

This revision also leaves the total predicted angular distributions used in fitting the data almost unchanged compared to simply adding the $\Delta T=0$ and $\Delta T=1$ angular distributions.

The angular distributions predicted for the SDR ($\Delta L=1$) and SQR ($\Delta L=2$) for $^{48}$Ca for $\omega_L=20$ MeV are shown in Fig. 8(b).

Finally, the present analysis differs from that for $^{40}$Ca in that for $^{44}$Ca and $^{48}$Ca contributions from $M1$ transitions are not negligible. Thus angular distributions were calculated for pure $(\nu f_{7/2})^n\rightarrow(\nu f_{7/2})^{n-1}(\nu f_{5/2})\ 1^+$ transitions where $n=4$ for $^{44}$Ca and $n=8$ for $^{48}$Ca; these were included in some of the $\chi^2$ minimization calculations as described in Sec. V. The predicted $1^+$ angular distribution ($\Delta L=0$) for $^{48}$Ca is shown in Fig. 8(b).

## V. RESULTS

### A. Results for $\sigma_0$

Since the details of how the calculations for $\sigma_0$ were done here differ from how the calculations for $^{40}$Ca were

done in Ref. [4], we have reanalyzed the $^{40}$Ca $\sigma_0$ as described in Sec. IV A so that all three isotopes can be meaningfully compared.

The results for the distributions of $\Delta L=1$, $\Delta S=0$, $\Delta T=1$ strength, the giant dipole resonance (GDR), are shown in Fig. 9. All three nuclei show a well-defined resonance near 20 MeV. At high $\omega$ the deduced strength is uniformly rising. It should be noted that, since the cross section for 100% EWSR at a given $\omega$ decreases like $\omega^{-1}$ as $\omega$ increases, this rise is not necessarily indicative of rising GDR cross section; in fact, the distributions of GDR cross sections for $\omega \geq 25$ MeV are approximately flat. Since this behavior has not been observed in any of the many experiments examining the GDR in nuclei, it certainly appears to be unphysical. Several possible explanations for this discrepancy exist: Fig. 4 shows that at high $\omega$, $\sigma_0$ is quite small and the results are therefore quite sensitive to the details of the analysis. A small instrumental background at small angles could result in extraction of too large strengths. Since momentum transfer increases with increasing $\omega$ for a given angle, if the predicted angular distributions were less accurate at larger momentum transfers (as might be expected where $\sigma_0$ becomes less dominated by Coulomb excitation), errors could be expected. It is also necessary to recall that our method of estimating $\sigma_0$ is only approximate and therefore particularly subject to errors when $\sigma_0 \ll \sigma_1$. In view of the difficulties at high $\omega$ we present here the summed strength up to 25 MeV: for $^{40}$Ca, (130±17)%; for $^{44}$Ca, (96±12)%; and for $^{48}$Ca, (157±14)%. The summed strength is substantially smaller for $^{44}$Ca; this could have been expected since, although $\sigma_{SF}$ is quite constant for all three nuclei as noted in Sec. III, Fig. 4 shows a substantially larger $\sigma_0$ for $^{48}$Ca than for $^{44}$Ca. In view of the fact that none of the summed GDR strengths are unreasonably large, our neglect of possible monopole transitions is probably justified. The reason for the anomalously low GDR strength in $^{44}$Ca is not understood.

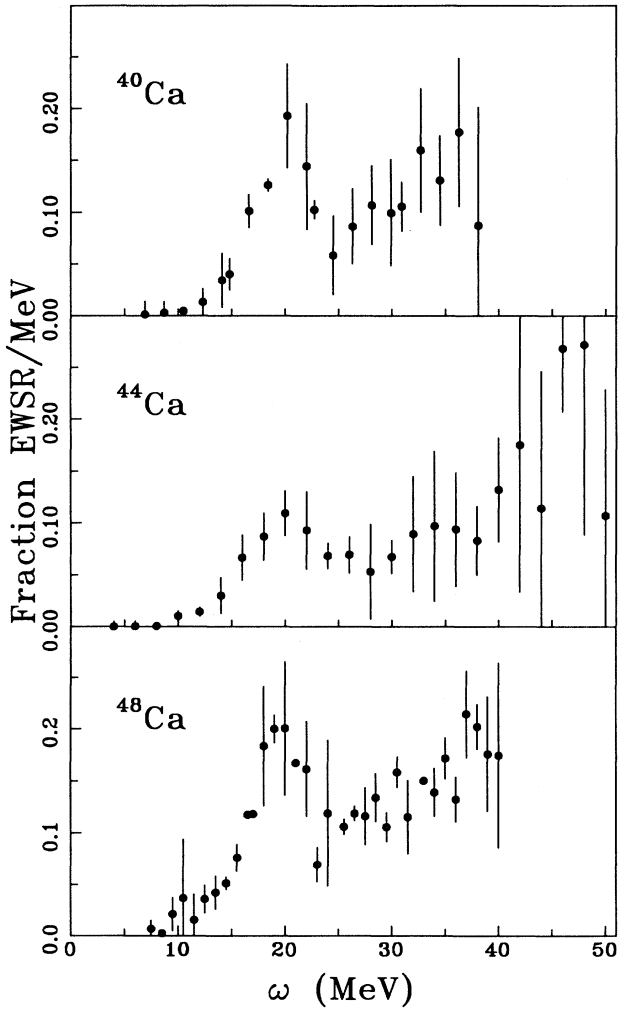


FIG. 9. Deduced distributions of $\Delta L=1$, $\Delta S=0$, $\Delta T=1$ strength, the giant dipole, for $^{40}$Ca, $^{44}$Ca, and $^{48}$Ca.

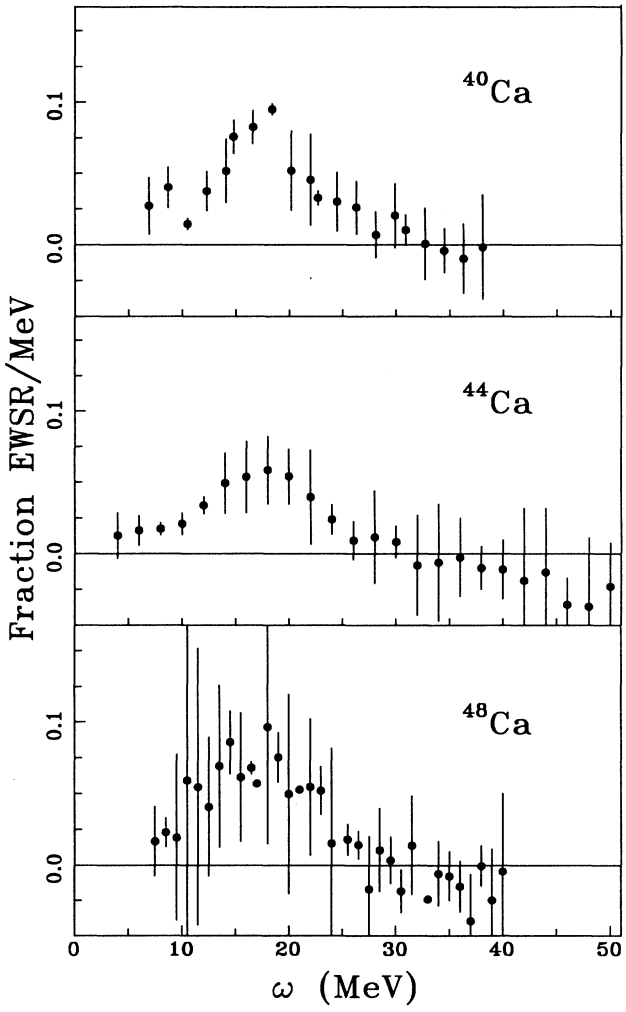


FIG. 10. Deduced distributions of $\Delta L=2$, $\Delta S=0$, $\Delta T=0$ strength, the giant quadrupole, for $^{40}$Ca, $^{44}$Ca, and $^{48}$Ca.

The results for the distributions of $\Delta L=2$, $\Delta S=0$, $\Delta T=0$ strength, the giant quadrupole resonances (GQR), are shown in Fig. 10. In all three isotopes a well-defined GQR peaked between 15 and 20 MeV is clearly seen. There is a tendency at high $\omega$ for the extracted strength to be negative indicating again, as suggested above, that the solutions for the multipole decompositions of $\sigma_0$ are unphysical at higher $\omega$. The very large uncertainties for $^{48}$Ca are due to the restricted angular range of the data ($\theta \leq 9°$). The summed strengths for 10 MeV $\leq \omega \leq 25$ MeV are for $^{40}$Ca, (86±11)%; for $^{44}$Ca, (68±12)%; and for $^{48}$Ca, (89±27)%. Within the uncertainties, these are all comparable although there is an indication that, as is the case for the GDR strength the GQR strength for $^{44}$Ca may be smaller.

### B. Results for $\sigma_{SF}$

Since our data extend only in to 3°, determination of $\Delta L=0$ strength is difficult, particularly in the region of strong spin-dipole strength. As $\omega$ increases, $q$ at a given scattering angle also increases thereby rendering this determination increasingly difficult at high excitation energies. After numerous exploratory calculations it was decided that the $\Delta L=0$ angular distribution should be included in the $\chi^2$ minimization searches only for $\omega < 20$ MeV; for larger $\omega$, nearly all searches yield $\Delta L=0$ strengths consistent with zero and with large errors and $\Delta L=1$ strengths with significantly larger uncertainties than obtained without the $\Delta L=0$ angular distribution included.

Shown in Fig. 11 are the distributions of $M1$ strength [as fractions of the $(\nu f_{7/2})^n \rightarrow (\nu f_{7/2})^{n-1}(\nu f_{5/2})$ DWIA cross sections] for $^{44}$Ca and $^{48}$Ca. For $^{48}$Ca there is little evidence of $M1$ strength other than in the well-known 10.23-MeV $1^+$ state; our measured strength for this state, (30±3)%, is in good agreement with previous measurements [14,15,24]. For $^{44}$Ca the deduced $M1$ strength is not concentrated in an isolated state but is fragmented among many states. We find, for 7 MeV $\leq \omega < 11$ MeV, (36±9)% of the $(\nu f_{7/2})^4 \rightarrow (\nu f_{7/2})^3(\nu f_{5/2})$ predicted total cross section in good agreement with previous high-resolution $(p,p')$ measurements [25]. For 7 MeV $\leq \omega \leq 13$ MeV, (53±12)% of this cross section is observed in good agreement with $(e,e')$ results [26]. Above 13 MeV the uncertainties become large; the total $M1$ strength measured for $\omega < 19$ MeV is (94±30)%.

Figure 12 shows the deduced spin-dipole strength distributions for $^{40}$Ca, $^{44}$Ca, and $^{48}$Ca. The distributions of spin-dipole strengths are qualitatively similar for all three nuclei. The summed spin-dipole strengths (for $\omega < 40$ MeV) are (160±19)% for $^{44}$Ca and (156±15)% for $^{48}$Ca. Since the $^{40}$Ca summed strength [5] is (154±17)%, the

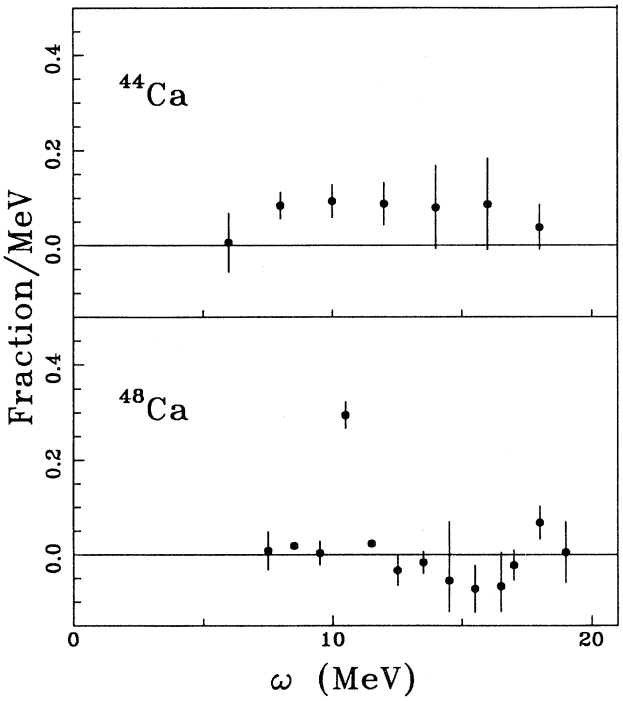


FIG. 11. Deduced distributions of $\Delta L=0$, $\Delta S=1$, strength, the $M1$, for $^{44}$Ca, and $^{48}$Ca.

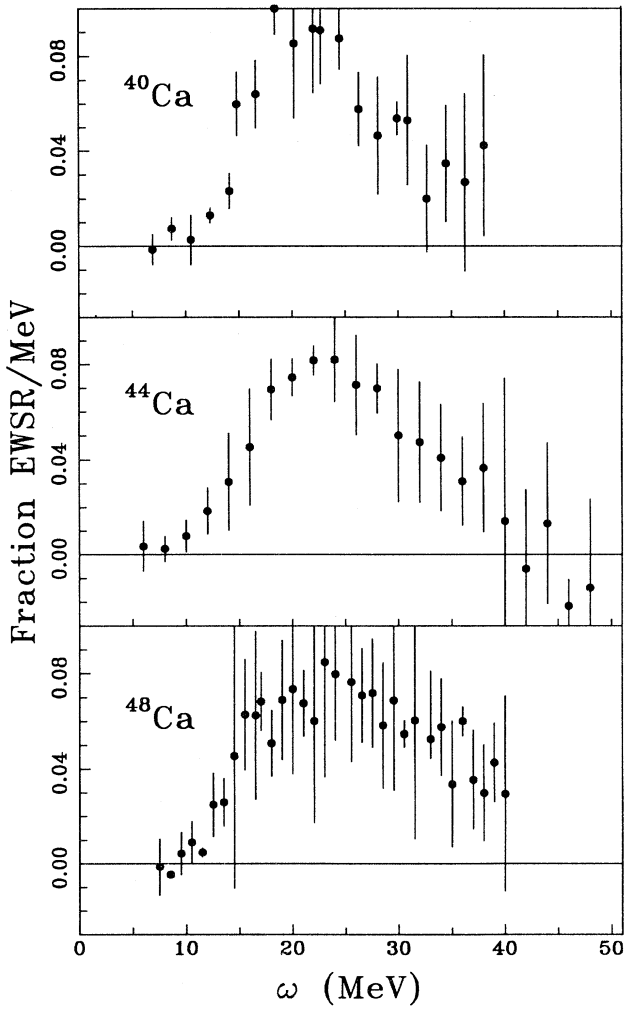


FIG. 12. Deduced distributions of $\Delta L=1$, $\Delta S=1$ strength, the spin dipole, for $^{40}$Ca, $^{44}$Ca, and $^{48}$Ca.

TABLE I. Summed strengths determined in the present work and in Ref. [2]. The strength units are, except for $\Delta L=0$, percentage of the EWSR. For $\Delta L=0$ the strength units are percentage of the DWIA predictions for the $(\nu f_{7/2})^n \rightarrow (\nu f_{7/2})^{n-1}(\nu f_{5/2})$ transitions.

| $\Delta L$ | $\Delta S$ | $\Delta T$ | Target | Integration range (MeV) | Strength |
|---|---|---|---|---|---|
| 1 | 0 | 1 | $^{40}$Ca | 6–25.4 | 130(17) |
| 1 | 0 | 1 | $^{44}$Ca | 3–25 | 96(12) |
| 1 | 0 | 1 | $^{48}$Ca | 7–25 | 157(14) |
| 2 | 0 | 0 | $^{40}$Ca | 9.6–25.4 | 86(11) |
| 2 | 0 | 0 | $^{44}$Ca | 9–25 | 68(12) |
| 2 | 0 | 0 | $^{48}$Ca | 10–25 | 89(27) |
| 0 | 1 | $\nu$ | $^{44}$Ca | 7–11 | 36(9) |
| 0 | 1 | $\nu$ | $^{44}$Ca | 7–13 | 53(12) |
| 0 | 1 | $\nu$ | $^{44}$Ca | 7–19 | 94(30) |
| 0 | 1 | $\nu$ | $^{48}$Ca | 9.5–10.5 | 29(3) |
| 1 | 1 | 1+0 | $^{40}$Ca | 6–38.9 | 154(17) |
| 1 | 1 | 1+0 | $^{44}$Ca | 3–41 | 160(19) |
| 1 | 1 | 1+0 | $^{48}$Ca | 7–40.5 | 156(15) |
| 2 | 1 | 1+0 | $^{40}$Ca | 6–38.9 | 256(26) |
| 2 | 1 | 1+0 | $^{44}$Ca | 3–41 | 235(26) |
| 2 | 1 | 1+0 | $^{48}$Ca | 7–40.5 | 155(24) |

total spin-dipole strength is quite independent of $A$ across the calcium isotopes (as could have been predicted from the constancy of $\sigma_{SF}$ at 5°). As noted in Ref. [5], one expects the Suzuki sum rule to underestimate the total strength since meson-exchange contributions are not included. One can therefore argue that a large fraction of the total spin-dipole strength is concentrated in a broad, collective resonance peaked near $\omega=20$ MeV. In $^{40}$Ca Horen *et al.* [27] observed significant quenching of spin-dipole strength; however, they only observed strength in the region $13\leq\omega\leq18$ MeV. Shell-model calculations [28] including coupling to two-particle–two-hole ($2p$-$2h$) excitations accounted for this quenching. The missing strength is just pushed up to higher $\omega$ by $2p$-$2h$ mixing; hence, the fact that we observe most of the spin-dipole strength in the region $\omega\leq40$ MeV could be consistent with the results of Ref. [27].

The distributions of spin-quadrupole strength suggested from the multipole analysis are shown in Fig. 13. The summed strengths, for $\omega\leq40$ meV, are (235±26)% for $^{44}$Ca and (155±24)% for $^{48}$Ca; they may be compared to the $^{40}$Ca results [5] of (256±26)%. These uncertainties depend on the statistical errors of the data and the search errors, but there are additional uncertainties as discussed below. We see no evidence for a predicted [29] large increase in spin-quadrupole strength for $^{48}$Ca. [It should be noted that this prediction is for $(p,n)$ cross sections, but the arguments seem equally applicable to $\sigma_{SF}$ for proton scattering.]

The spin-quadrupole strength distributions must be taken less seriously than those for the SDR because, primarily of the neglect of higher multipoles in our analyses. In addition, the approximations used to simulate the effects of distortions may be less reliable than for the spin-dipole transitions [5]. Another possible contributor to apparent spin-quadrupole strength might be spin-monopole transitions [30]. Boucher has recently shown [31] that, in the schematic model, the angular distribu-

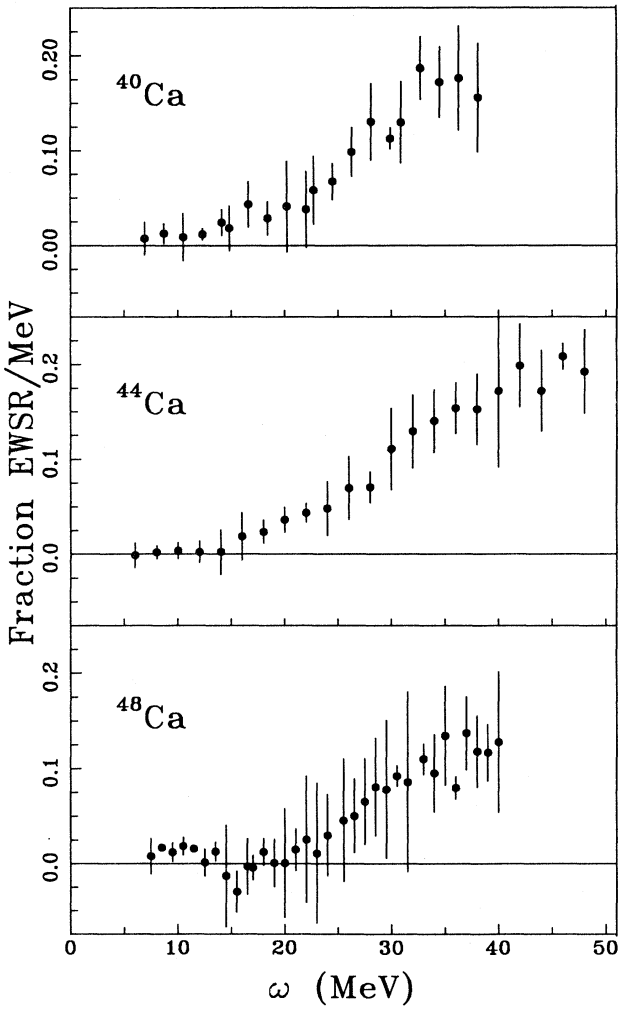


FIG. 13. Deduced distributions of $\Delta L=2$, $\Delta S=1$ strength, the spin quadrupole, for $^{40}$Ca, $^{44}$Ca, and $^{48}$Ca.

tion for a spin-monopole transition would be indistinguishable from that of a spin-quadrupole transition; we have performed DWIA calculations for the $1d \rightarrow 2d$, $\Delta S=1$, $\Delta L=0$, $\Delta T=1$ transition in $^{40}$Ca and find, indeed, a strong peak in the predicted angular distribution near 10° which is near where the spin-quadrupole angular distribution peaks. To determine more accurately the distribution of spin-quadrupole strength and to study higher multipole strengths will require acquisition of data for larger angles, but even this will probably not resolve the spin-quadrupole strength from possible spin-monopole strength.

## VI. CONCLUSIONS

The summed multipole strengths determined for the calcium isotopes are summarized in Table I. For $^{48}$Ca, we have found no evidence for $M1$ strength other than in the well-known 10.23-MeV $1^+$ state. In $^{44}$Ca, $M1$ strength was observed to be distributed from 7 to 13 MeV with some indication that strength may extend to higher $\omega$. The spin-dipole resonances in $^{44}$Ca and $^{48}$Ca are very similar to the spin-dipole resonance previously observed in $^{40}$Ca: all three nuclei have a resonance, centered near $\omega=20$ MeV and a width of about 20 MeV, which exhausts approximately 150% of the Suzuki sum rule [22]. Results for the spin-quadrupole resonance must be considered unreliable due to probable contributions from other multipoles.

The analysis of $\sigma_0$, the approximate cross sections for $\Delta S=0$ transitions, yielded a summed strength for the GDR in $^{44}$Ca which was significantly smaller than the corresponding summed strengths for $^{40}$Ca and $^{48}$Ca; similarly, the GQR is somewhat less strongly excited in $^{44}$Ca.

## ACKNOWLEDGMENTS

This work was supported in part by the United States Department of Energy, The National Science Foundation, and the Natural Sciences and Engineering Research Council of Canada.

[1] C. Glashausser, K. Jones, F. T. Baker, L. Bimbot, H. Esbensen, R. W. Fergerson, A. Green, S. Nanda, and R. D. Smith, Phys. Rev. Lett. **58**, 2404 (1987).
[2] F. T. Baker, L. Bimbot, B. Castel, R. W. Fergerson, C. Glashausser, A. Green, O. Häusser, K. Hicks, J. Jones, C. A. Miller, S. K. Nanda, R. D. Smith, M. Vetterli, J. Wambach, R. Abegg, D. Beatty, V. Cupps, C. Djalali, R. Henderson, K. P. Jackson, R. Jeppesen, J. Lisantti, M. Morlet, R. Sawafta, W. Unkelbach, A. Willis, and S. Yen, Phys. Lett. B **237**, 337 (1990).
[3] L. Bimbot, R. W. Fergerson, C. Glashausser, K. W. Jones, F. T. Baker, D. Beatty, V. Cupps, A. Green, and S. Nanda, Phys. Rev. C **42**, 2367 (1990).
[4] F. T. Baker, L. Bimbot, R. W. Fergerson, C. Glashausser, K. Jones, A. Green, K. Nakayama, and S. Nanda, Phys. Rev. C **37**, 1350 (1988).
[5] F. T. Baker, L. Bimbot, R. W. Fergerson, C. Glashausser, A. Green, K. Jones, W. G. Love, and S. Nanda, Phys. Rev. C **40**, 1877 (1989).
[6] O. Häusser, M. C. Vetterli, R. W. Fergerson, C. Glashausser, R. G. Jeppesen, R. D. Smith, R. Abegg, F. T. Baker, A. Celler, R. L. Helmer, R. Henderson, K. Hicks, M. J. Iqbal, K. P. Jackson, K. W. Jones, J. Lisantti, J. Mildenberger, C. A. Miller, R. S. Sawafta, and S. Yen, Phys. Rev. C **43**, 230 (1991).
[7] W. Unkelbach and J. Wambach, private communication.
[8] W. G. Love and M. A. Franey, Phys. Rev. C **24**, 1073 (1981).
[9] M. A. Franey and W. G. Love, Phys. Rev. C **31**, 488 (1985).
[10] R. S. Henderson, O. Häusser, K. Hicks, G. Günther, W. Faszer, R. Sawafta, and N. Poppe, Nucl. Instrum. Methods **A254**, 61 (1987).
[11] O. Häusser, R. S. Henderson, K. Hicks, D. A. Hutcheon, D. Clark, C. Günther, R. Sawafta, and G. W. Waters, Nucl. Instrum. Methods **A254**, 67 (1987).
[12] R. Fergerson, J. McGill, C. Glashausser, S. Nanda, Sun Zuxun, M. Barlett, G. Hoffmann, J. Marshall, and J. McClelland, Phys. Rev. C **38**, 2193 (1988).
[13] D. J. Horen, F. E. Bertrand, E. E. Gross, T. P. Sjoreen, D. K. McDaniels, J. R. Tinsley, J. Lisantti, L. W. Swenson, J. B. McClelland, T. A. Carey, S. J. Seestrom-Morris, and K. Jones, Phys. Rev. C **30**, 709 (1984).
[14] D. J. Horen, F. E. Bertrand, E. E. Gross, T. P. Sjoreen, D. K. McDaniels, J. R. Tinsley, J. Lisantti, L. W. Swenson, J. B. McClelland, T. A. Carey, S. J. Seestrom-Morris, and K. Jones, Phys. Rev. C **31**, 2049 (1985).
[15] S. K. Nanda, C. Glashausser, K. W. Jones, J. A. McGill, T. A. Carey, J. B. McClelland, J. M. Moss, S. J. Seestrom-Morris, J. R. Comfort, S. Levenson, R. Segel, H. Ohnuma, Phys. Rev. C **29**, 660 (1984).
[16] B. D. Anderson, T. Chittrakarn, A. R. Baldwin, C. Lebo, R. Madey, P. C. Tandy, J. W. Watson, B. A. Brown, and C. C. Foster, Phys. Rev. C **31**, 1161 (1985).
[17] G. F. Bertsch and S. F. Tsai, Phys. Rep. **18**, 125 (1975).
[18] Y.-W. Liu, J. D. Bronson, C. M. Rozsa, D. H. Youngblood, P. Bogucki, and U. Garg, Phys. Rev. C **24**, 884 (1981).
[19] F. R. Bertrand, G.R. Satchler, D. J. Horen, and A. van der Woude, Phys. Lett. **80B**, 198 (1975).
[20] P. M. Boucher, B. Castel, K. Okuhara, I. P. Johnstone, J. Wambach, and T. Suzuki, Phys. Rev. C **37**, 906 (1988).
[21] J. B. Bellicard, P. Bounin, R. F. Frosch, R. Hofstadter, J. S. McCarthy, F. J. Uhrhane, M. R. Yearian, B. C. Clark, R. Herman, and D. G. Ravenhall, Phys. Rev. Lett. **19**, 527 (1967).
[22] T. Suzuki, Ann. Phys. (Paris) **9**, 535 (1984).
[23] T. Suzuki, Phys. Lett. **83B**, 147 (1979).
[24] G. M. Crawley, N. Anantaraman, A. Galonsky, C. Djalali, N. Marty, M. Morlet, A. Willis, and J.-C. Jourdain, Phys. Lett. **127B**, 322 (1983).
[25] C. Djalali, thesis, University of Paris, 1984.
[26] A. Richter, Cours de Physique Nucléaire, Février 84-ALS CEA Saclay.

[27] D. J. Horen, J. Lisantti, R. L. Auble, F. E. Bertrand, B. L. Burks, E. E. Gross, R. O. Sayer, D. K. McDaniels, K. W. Jones, J. B. McClelland, S. J. Seestrom-Morris, and L. W. Swenson, Z. Phys. A **333**, 39 (1989).
[28] P. M. Boucher and B. Castel, Phys. Rev. C **41**, 786 (1990).
[29] F. Osterfeld, Phys. Rev. C **26**, 762 (1983).
[30] N. Auerbach and A. Klein, Phys. Rev. C **30**, 1032 (1984).
[31] P. M. Boucher, preprint.